LAB 01

All the images in this lab was collected either from the personal album or from the website. All of them were colored images and then converted into gray-scale images by MATLAB. In figure 1(a), the corn seeds are an example of a collection of small objects while in figure 1(b) the sweets resemble a collection of large objects. The fireworks in figure 1 (c) is an example of directionally oriented features where the fireworks scatter from a center point. The picture of a piece of cloth in figure 1(d) is an example of fine texture.


(a)

(b)

(c)

(d)

Figure 1: (a) A collection of small objects; (b) A collection of large objects; (c) Directional(oriented) features; (d) Fine texture
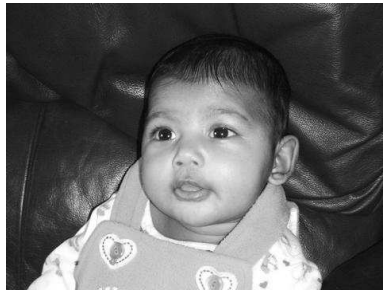
The crack in the road in figure 2(a) represents the coarse texture while the pyramid in figure 2(b) is a geometrical shape.The figure 2(c) shows a baby face. The waves of the sea in figure 2(d) is a smooth feature.The building in figure 2(e) shows the sharp edges and the railing of a balcony in figure 2(f) is a kind of periodic pattern.

(a)
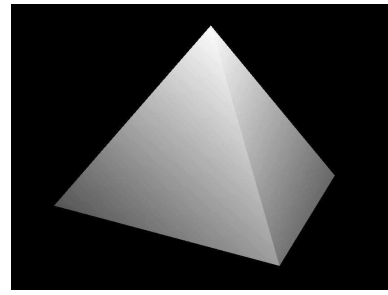
(b)

(c)

(d)

(e)

(f)

Figure 2: (a) Coarse texture; (b) Geometrical shapes; (c)Human face; (d) Smooth features; (e) Sharp edges; (f) Periodic patterns

LAB 02

The image in figure 1(a) is a collection of corn seeds. Figure 1(b) and 1(c) show the histogram and the log magnitude Fourier spectrum of figure 1(a) respectively. It is seen in the histogram that most of the pixels in the image lie within the range of 50-220. It is evident from the image that it does not have any dark background to have gray levels near to 0. The corn seeds are uniformly distributed over the whole image and giving the medium gray levels. The image is almost unimodal, that is, it has only one major peak around 140 and has the shape of a gaussian. In the Fourier spectrum, the large amount of energy is concentrated at the center at DC, but still some energies are distributed over a large band of frequencies.

Figure 1(d) is a building with sharp edges. The histogram in figure 1(e) is almost available over the whole range of gray levels of 0-255. The first peak around 50 is due to the dark windows of the building. The last prominent peak at about 225 is due to the brighter background of the image. The gray levels ranging from 120-200 are due to other different shades present in the whole building and background. The Fourier spectrum in figure 1(f) shows different lines through the center for different sharp edges present in the image. The lines from the lower left portion of the spectrum to the upper right is due to the top edge and parallel bars present across the building. The other line from left to right is due to the vertical edges.

The fireworks in figure 1(g) is an example of the directional feature. The highest peak at around 5 in the histogram of figure 1(h) is due to the dark black background of the image. The few gray levels from 240-255 due to the bright radiating lights of fireworks. The Fourier spectrum in figure 1(i) clearly exhibits the directional nature of the image. The radiating lines from the center correspond to the omnidirectional orientation. Though a large portion of energies are around the low frequency region for the uniform background without intrinsic changes; due to sharp changes from the dark background to the bright lights high frequency components are also seen in the spectrum.

The histogram and the log magnitude Fourier spectrum of the figure 2(a) is given by the figures 2(b) and 2(c) respectively. The histogram spans the whole range of gray levels from 0-255 as it is evident from the image that all shades of gray levels are present in the feature. But the highest portion of gray levels are present within the range of 100-200. The peaks around 150-200 is for the road. In the Fourier spectrum, most of the energy is centered at DC and there is a vertical line along the center for the horizon at far end of the image.

The waves in figure 2(d) is an example of smooth features. The histogram in figure 2(e) has a smooth unimodal peak. The histogram range from 70-255 while most of the gray levels are within 100-200. The few gray levels near 255 is due to the bright waves. The Fourier spectrum in figure 2(f) shows most of the energy at the center. There are some frequencies in the vertical direction due to the sharp edges of the waves.

The pyramid in the figure 2(g) is a kind of geometrical patterns consisting of triangles. In figure 2(h), the histogram shows a high peak around 0 due to the large black background. The other gray levels ranging from 80-220 represents the various shades of the pyramid. The Fourier spectrum in figure 2(i) shows all the lines corresponding to the different edges of the triangles. For example the left edge of the pyramid corresponds to the line from top left to lower right corner in the spectrum.
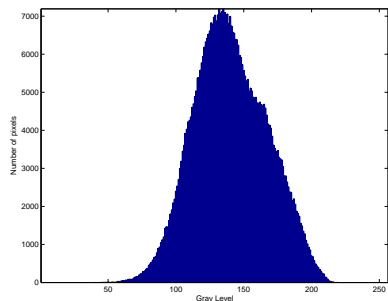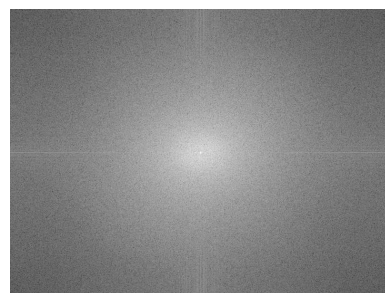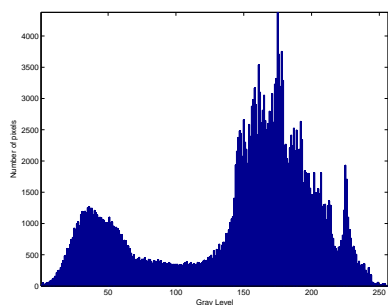
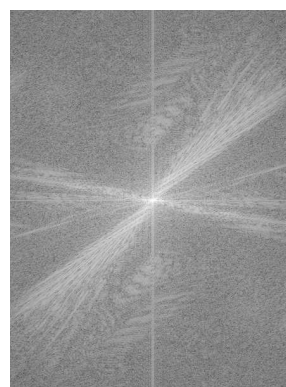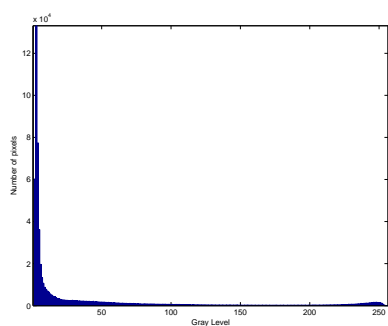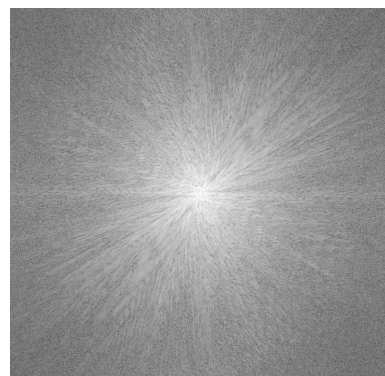Figure 1: (a) Small objects; (b) Histogram of gray levels in (a); (c) Fast-Fourier Transform of(a); (d) Sharp edges; (e)Histogram of gray levels in (d); (f) Fast-Fourier Transform of (d); (g) Directional feature; (h) Histogram of gray levels in (g); (i) Fast-Fourier Transform of (g) .
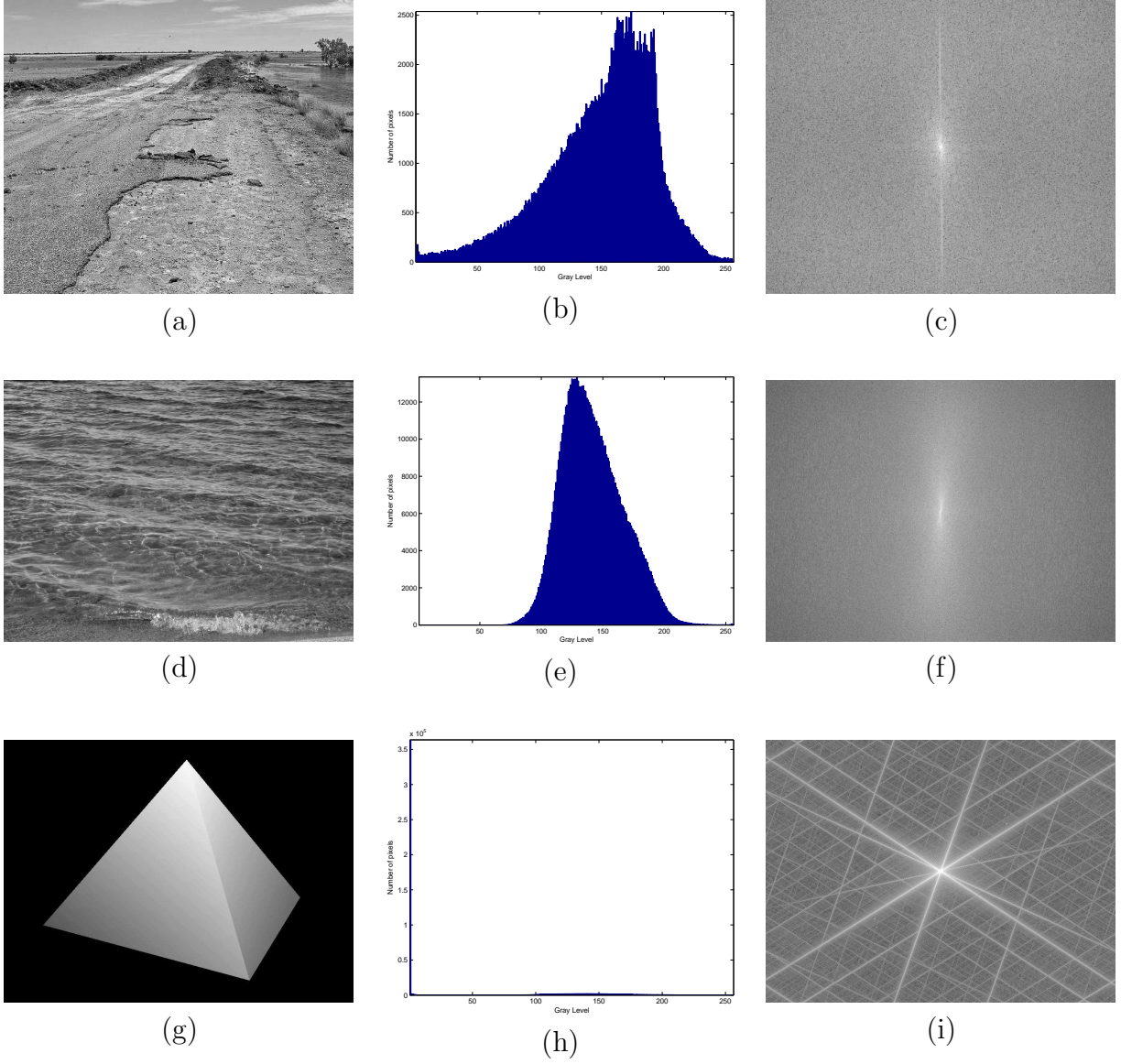
Figure 2: (a) Coarse texture; (b) Histogram of gray levels in (a); (c) Fast-Fourier Transform of(a); (d) Smooth features; (e) Histogram of gray levels in (d); (f) Fast-Fourier Transform of (d); (g) Geometrical shape; (h) Histogram of gray levels in (g); (i) Fast-Fourier Transform of (g).

LAB 03

Figure 1(a) represents a test image of size 100 x 100 pixels with a circle of diameter 30 pixels at the center of the image. Figure 1(b), 1(c) and 1(d) show three blurred versions of the test image by applying the 3 x 3 mean filter once, three times and five times respectively. Though the shape of the circle is still recognizable, it is seen that, the increasing number of 3 x 3 mean filtering has degraded the quality of the original image by blurring the edges. The original uneven shape of the circle has been made smooth by blurring its edges.

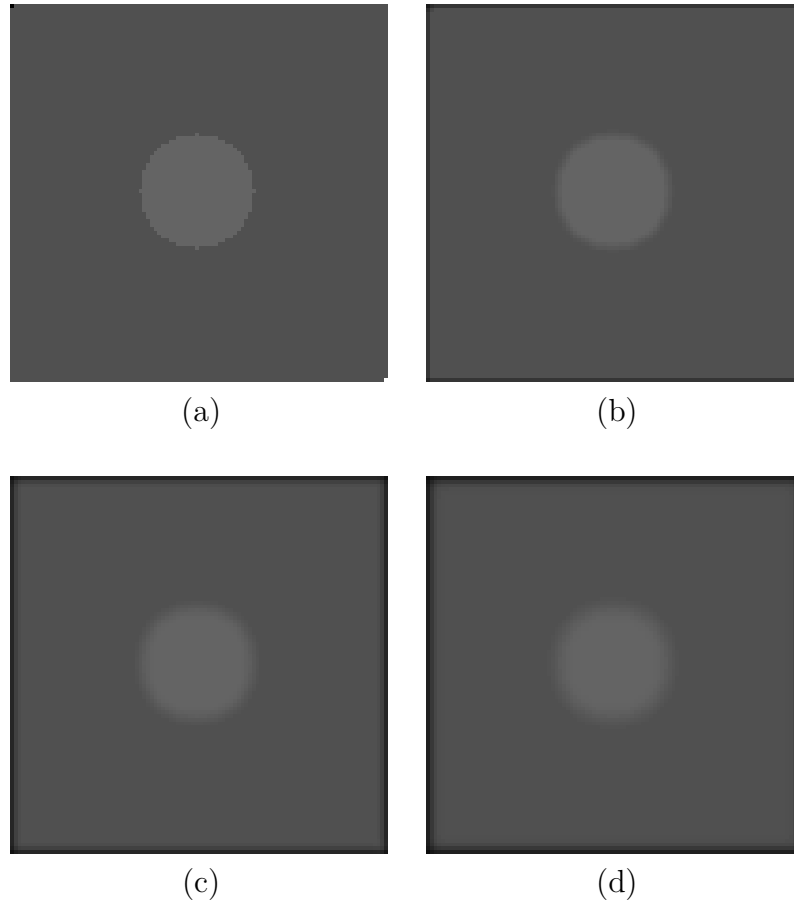

(a)   (b)

(c)   (d)

Figure 1: (a) Original test image of size 100 x 100 pixels. (b) Original image filtered once by 3x3 mean filter. (c) Original image filtered three times by 3x3 mean filter. (d) Original image filtered five times by 3x3 mean filter.

Figure 2 shows the effect of applying three levels of Gaussian noise to the three blurred images of Figure 1. It can be easily seen that the worst perceptible image corresponds to the image with the highest level of additive noise and the greatest number of iterations of the filter. Table 1 shows

the various values of MSE and NMSE for different iterations of the mean filter and for increasing noise. Examining Table 1, the mean-square errors clearly show that with increasing noise and with increasing iterations of the 3x3 mean filter, the image quality degrades quickly.

For example, in Table 1, for a normalized variance of noise, σ^2=0.0001, the MSE for one iteration of the mean filter is 34.21, and quickly increases to 128.11 with five iterations of the mean filter. Similarly, for five applications of the filter and a normalized noise variance of σ^2=0.0001, the MSE is 128.11 and increases with higher levels of noise to 223.89 for a variance of σ^2=0.01.

Although the various levels of noise and the different number of iterations of the mean filter affect the MSE accordingly, there is also another artifact in the images which contribute to the image errors. When applying a mean filter mask to the image, it is zero-padded close to the edges. This causes a false representation of the data around the edges and results in the black visible border in case of all the filtered images. This effects the MSE results, compounding the errors due to the noise and effects of blurring. In order to obtain a more accurate result of the MSE, the border could be eliminated in the calculation of the error.

The application of the 3x3 mean filter five times represents the worst-case in terms of image quality and is shown in Figure 1(d). In the cases of relatively low levels of noise (Figure 2 (a), (d), (g)), the effects are barely perceptible. The object is still distinguishable from the background and is consistently blurred like the filtered images. In the presence of higher levels of noise (σ^2=0.01), the images in figure 2(c), (f) and (i) are degraded such that it is difficult to distinguish the object's edges. The core of the object is still clear; however, the edges are both blurred and noisy, making it complicated to identify the object's exact boundaries.

Figure 3 shows the effect of applying three levels of Speckle noise to the three blurred images of Figure 1. The effect of adding noise is same as described above. Table 2 shows the various values of MSE and NMSE for different level of noise and filter iteration. The mean-square errors increase with increasing noise and increasing iterations of the 3x3 mean filter.

For example, in Table 2, for a normalized variance of noise, σ^2=0.0001, the MSE for one iteration of the mean filter is 33.85, and quickly increases to 127.87 with five iterations of the mean filter. Similarly, for five applications of the filter and a normalized noise variance of σ^2=0.0001, the MSE is 127.87 and increases with higher levels of noise to 188.54 for a variance of σ^2=0.01.

Mean Filtering	$\sigma_\eta^2 = 0.0001$		$\sigma_\eta^2 = 0.001$		$\sigma_\eta^2 = 0.01$	
	MSE	NMSE	MSE	NMSE	MSE	NMSE
Once	34.21	0.005	42.99	0.006	124.69	0.018
Three times	85.85	0.012	94.42	0.014	181.23	0.027
Five times	128.11	0.019	135.26	0.020	223.89	0.033

Table 1: MSE and NMSE for images with Gaussian Noise

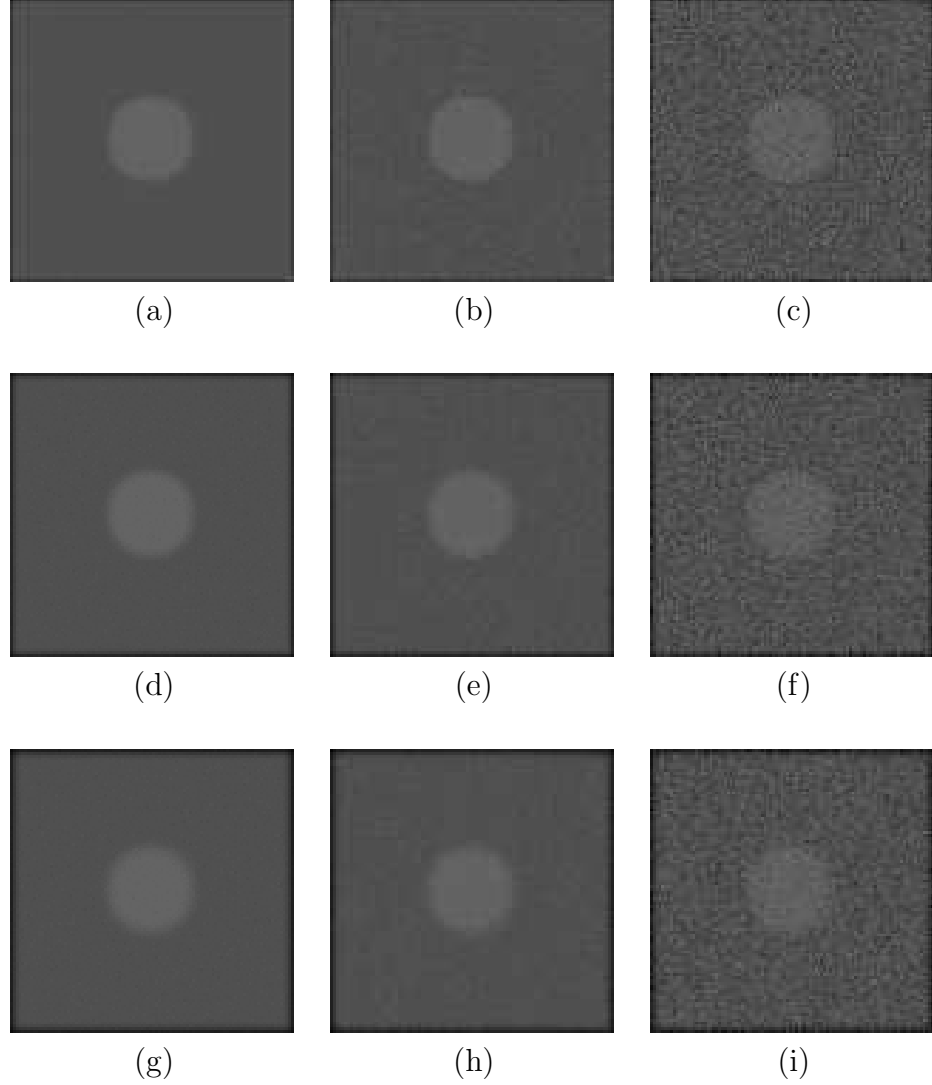| Mean Filtering	$\sigma_\eta^2 = 0.0001$		$\sigma_\eta^2 = 0.001$		$\sigma_\eta^2 = 0.01$	
	MSE	NMSE	MSE	NMSE	MSE	NMSE
Once	33.85	0.005	39.55	0.005	94.72	0.014
Three times	85.23	0.012	90.34	0.013	147.15	0.022
Five times	127.87	0.019	133.08	0.019	188.54	0.028

Table 2: MSE and NMSE for images with Speckle Noise

Figure 2: Gaussian noise applied to the test image that is filtered once by 3x3 mean filter(a) For $\mu=0$,normalized $\sigma^2=0.0001$; (b) For $\mu=0$,normalized $\sigma^2=0.001$; (c) For $\mu=0$,normalized $\sigma^2=0.01$; Gaussian noise applied to the test image that is filtered three times by 3x3 mean filter (d) For $\mu=0$,normalized $\sigma^2=0.0001$; (e) For $\mu=0$,normalized $\sigma^2=0.001$; (f) For $\mu=0$,normalized $\sigma^2=0.01$; Gaussian noise applied to the test image that is filtered five times by 3x3 mean filter (g) For $\mu=0$,normalized $\sigma^2=0.0001$; (h) For $\mu=0$,normalized $\sigma^2=0.001$; (i) For $\mu=0$,normalized $\sigma^2=0.01$
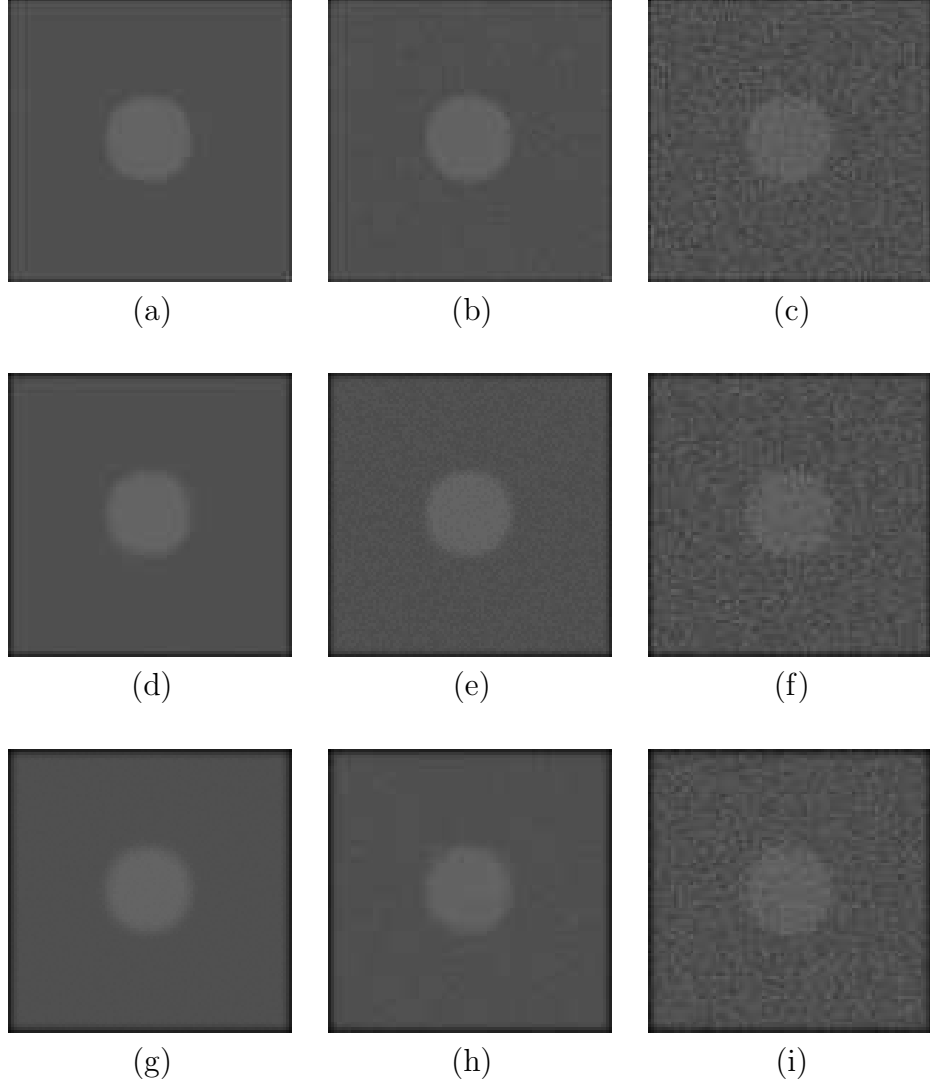
Figure 3: Speckle noise applied to the test image that is filtered once by 3x3 mean filter(a) For $\mu=0$,normalized $\sigma^2=0.0001$; (b) For $\mu=0$,normalized $\sigma^2=0.001$; (c) For $\mu=0$,normalized $\sigma^2=0.01$; Speckle noise applied to the test image that is filtered three times by 3x3 mean filter (d) For $\mu=0$,normalized $\sigma^2=0.0001$; (e) For $\mu=0$,normalized $\sigma^2=0.001$; (f) For $\mu=0$,normalized $\sigma^2=0.01$; Speckle noise applied to the test image that is filtered five times by 3x3 mean filter (g) For $\mu=0$,normalized $\sigma^2=0.0001$; (h) For $\mu=0$,normalized $\sigma^2=0.001$; (i) For $\mu=0$,normalized $\sigma^2=0.01$

LAB 04

Figure 1(a) is a test image of a building with strong edges and features. Figure 2(a) is a test image of sea waves with weaker definition of edges and features. Differentiation of an image results in extraction of edges and highpass filtering. It is seen that the two derivatives in horizontal and vertical direction extract edges in the corresponding directions; edges in the direction orthogonal to that of the operator are removed. The Laplacian is an omnidirectional operator and detects edges in all directions.

The horizontal derivative was obtained by convolving the image with the mask $[-1, 1]$. The results are presented in part (b) of Figures 1 and 2. This operation detects edges that are not oriented horizontally in the image, as demonstrated in the figures.From figure 1(b), it is seen that horizontal derivative operation has detected all the vertical edges including the left and right corners of the building. From figure 2(b), it is seen that, the vertical parts of the wave has been detected.

The vertical derivative was obtained by convolving the image with $[-1, 1]^T$. The results are presented in part (c) of Figures 1 and 2. This operation detects edges that are not oriented vertically in the image, as demonstrated in figures. From figure 1(c), it is visible that the vertical derivative has detected the horizontal edges of the building including the edges of all the floors.

The Laplacian operation was obtained by convolving the image with the 3x3 mask

$$\begin{bmatrix} 0 & 1 & 0 \\ 1 & -4 & 1 \\ 0 & 1 & 0 \end{bmatrix}.$$

The results are presented in part (d) of Figures 1 and 2. The Laplacian operator detected edges in all directions as seen in the figures, but the results are less strongly emphasized than in the individual application of the horizontal and vertical derivate operators. It should be noted that, there is a slight disjoint border around the image in both the figures. This is due to the use of zero-padding in the regions of the border when the Laplacian operator is applied. The edges in both figures are still very clearly detected.
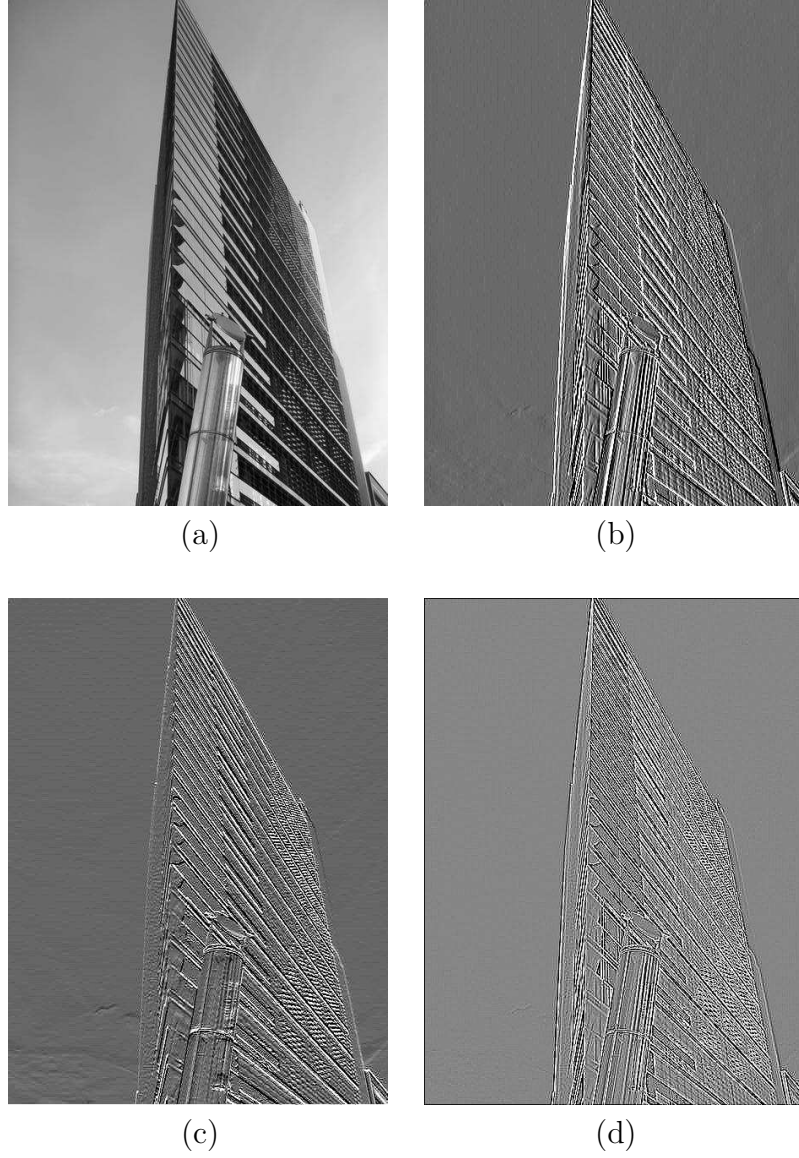
Figure 1: (a) A test image with strong edges; (b) The horizontal difference of image (a), display range [-17.5,24.4] out of [-175,244]; (c) The vertical difference of image (a), display range [-16.1,24] out of [-161,240]; (d) The Laplacian of image(a), display range [-55.6,50] out of [-556,500]
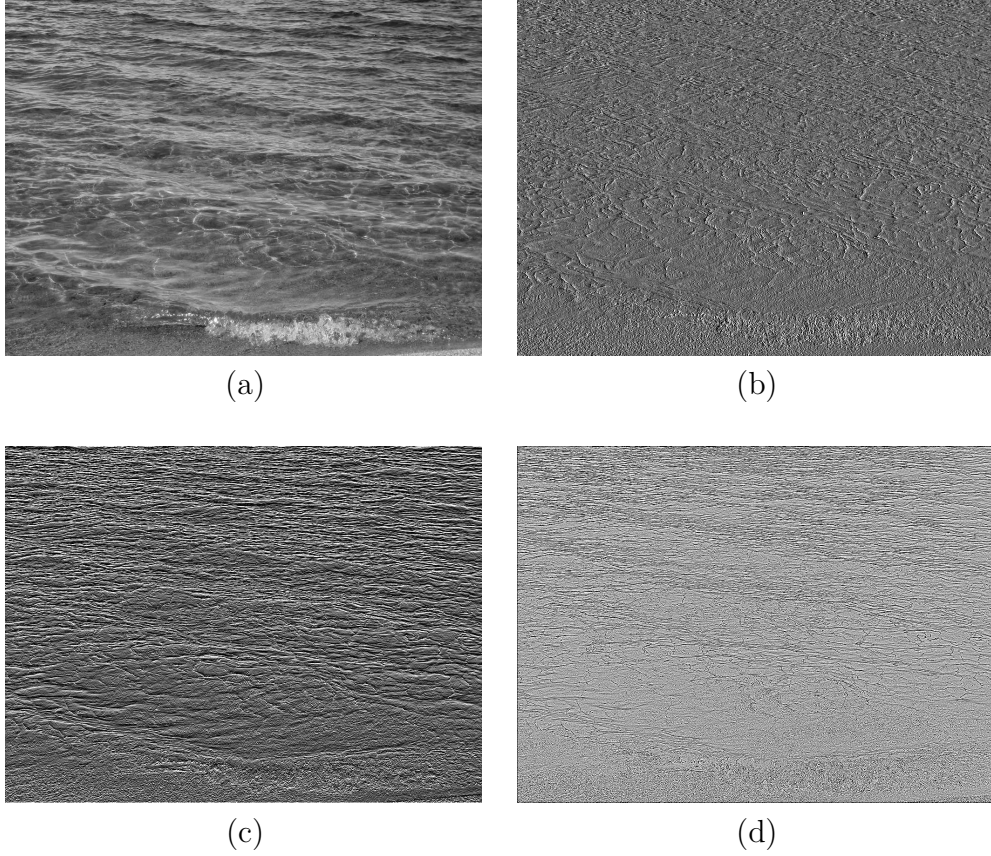
Figure 2: (a) A test image with weaker definition of edges; (b) The horizontal difference of image (a), display range [-13.7,20.3] out of [-137,203] ; (c) The vertical difference of image (a), display range [-12.4,23.2] out of [-124,232]; (d) The Laplacian of image(a), display range [-43.4,24.5] out of [-434,245]

LAB 05

Figure 1 and 2 represent the effect of applying three different neighborhood shapes of median filter and 3x3 mean filter into the noisy versions of an image with strong edges. In figure 1, gaussian noise is added to the original image. Though gaussian noise is not completely eliminated , the 3x3 square and 4-connected neighborhood median filter has minimized the noise and the sharp edges of the building are quite visible. In case of 5x5 square neighborhood median filter, the noise is more eliminated than the previous two. But it has completely eliminated the small objects. The 3x3 mean filter has reduced the gaussian noise but has blurred the sharp edges. From table 1, comparing the MSE it is seen that, the 3x3 square median filter performed the best while the 5x5 median filter performed the worst.

Type of Filter	MSE for Gaussian Noise	MSE for Salt-and-pepper Noise
Noisy image	615.67	998.64
3x3 Square median	257.26	138.35
4-Connected median	290.84	111.32
5x5 Square median	360.97	318.08
3x3 Mean	272.88	329.42

Table 1: Sharp edges: MSE for the noisy image, median and mean filtered image for Gaussian noise with $\mu=0$, normalized $\sigma^2=0.01$ and for Salt-and-pepper noise with normalized $\sigma^2=0.05$

Type of Filter	MSE for Gaussian Noise	MSE for Salt-and-pepper Noise
Noisy image	649.90	858.85
3x3 Square median	196.41	77.81
4-Connected median	231.93	35.74
5x5 Square median	203.78	153.48
3x3 mean	164.30	192.92

Table 2: Smooth edges: MSE for the noisy image, median and mean filtered image for Gaussian noise with $\mu=0$, normalized $\sigma^2=0.01$ and for Salt-and-pepper noise with normalized $\sigma^2=0.05$

In figure 2, salt-and-pepper noise is added to the original image. The 3x3 square median filter completely removed the noise without distorting the original image while 5x5 square median filter has removed the noise and has also distorted the image by eliminating all the small objects. The 4-connected median filter could not eliminate noise completely. The 3x3 mean filter has failed to remove most of the noise and has also blurred the sharp edges of the image. From table 1 in terms of MSE, we get that, 4 connected median filter has shown better performance than the other.

Figure 3 and 4 represent the effect of applying three different neighborhood shapes of median filter and 3x3 mean filter into the noisy versions of an image with weak edges and features. In figure 3, gaussian noise is added to the original image. All the median filters have performed relatively well in removing noise. While 5x5 square median filter has removed the noise more efficiently, it has also eliminated some small objects in the image. The mean filter has also removed the noise clearly, but has blurred some of the edges present in the image. From table 2, comparing the MSE, it is seen that the mean filter has shown the best performance. It is also evident from the nature of the mean filter that, the mean filter can remove noise from smooth images while in case of images with sharp edges, it results in blurring of edges and loss of fine details and texture.
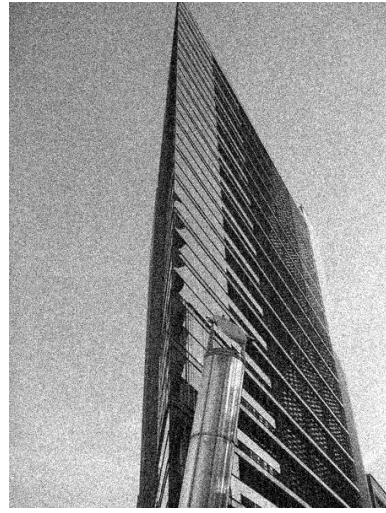
In figure 4 salt-and-pepper noise is added to the original image. All the median filters have removed the noise pretty well while mean filter failed to remove most of the noise. 5x5 square median filter has eliminated the small objects of the image. From table 2, it is seen that 4-connected median filter has got the best result while 3x3 mean filter has got the worst in terms of MSE.

So from the above discussion, we can come to a conclusion that, the median filter provides better noise removal than mean filter without blurring, especially when the noise has a long-tailed PDF and in the case of salt-and-pepper noise. However, the median filter could result in clipping of corners and distortion of the shape of sharp-edged objects. Median filtering with large neighborhoods could also result in the complete elimination of small objects.

Note: In case of the figure of the smooth features (figure 3 and 4), the result is clearly visible if the figures are magnified.
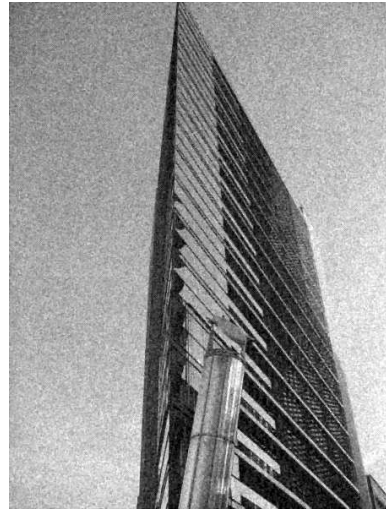
Figure 1: (a) Original image ; (b)Original image with Gaussian noise, normalized σ^2=0.01; Result of median filtering (c) using 3x3 square or 8-connected neighborhood; (d) using 4-connected neighborhood; (e) using 5x5 square; (f) Result of 3x3 mean filtering
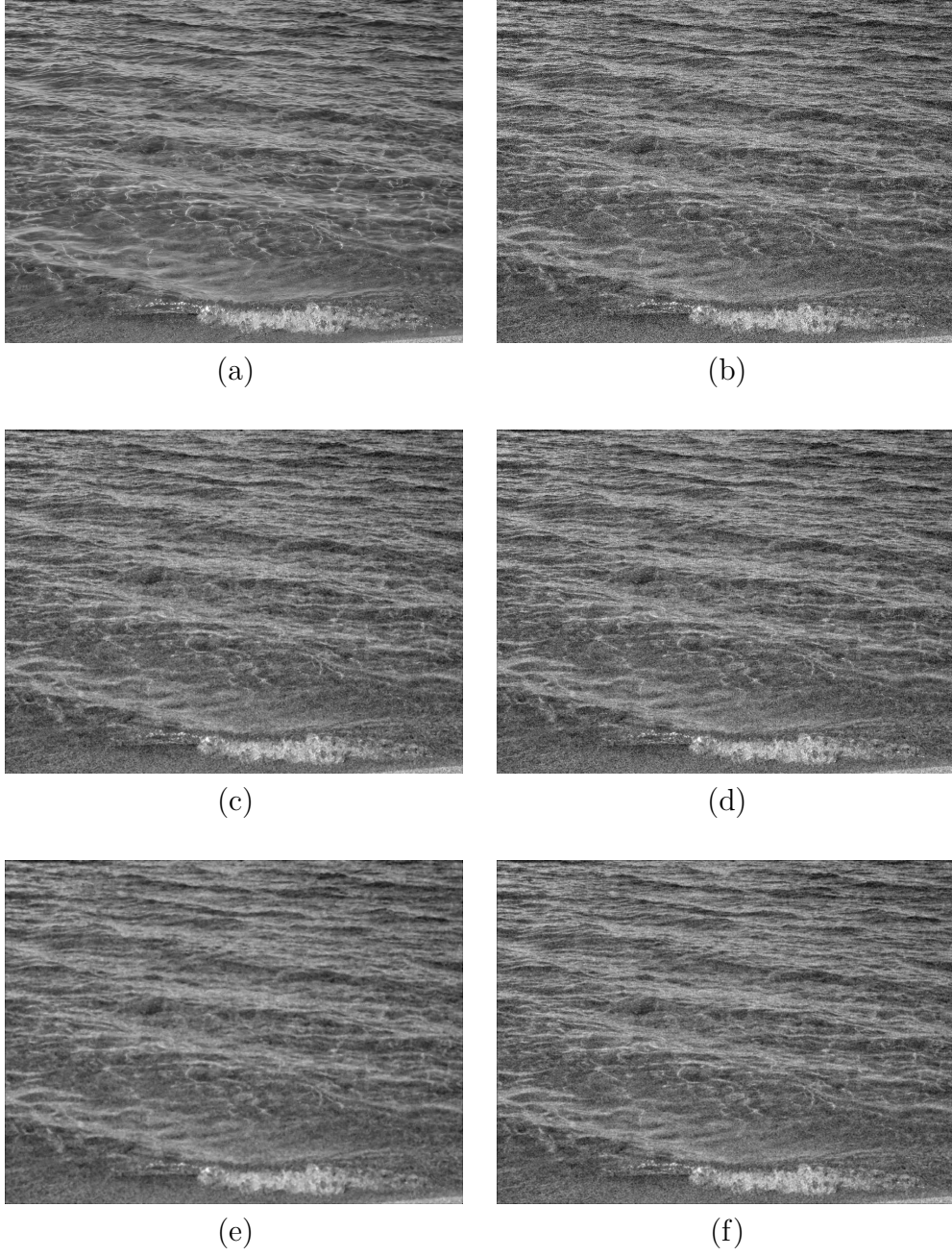
Figure 2: (a) Original image ; (b)Original image with Salt-and-Pepper noise, normalized σ^2=0.05; Result of median filtering (c) using 3x3 square or 8-connected neighborhood; (d) using 4-connected neighborhood; (e) using 5x5 square; (f) Result of 3x3 mean filtering

4

Figure 3: (a) Original image; (b)Original image with Gaussian noise, normalized σ^2=0.01; Result of median filtering (c) using 3x3 square or 8-connected neighborhood; (d) using 4-connected neighborhood; (e) using 5x5 square; (f) Result of 3x3 mean filtering

Figure 4: (a) Original image; (b)Original image with Salt-and-Pepper noise, normalized σ^2=0.05; Result of median filtering (c) using 3x3 square or 8-connected neighborhood; (d) using 4-connected neighborhood; (e) using 5x5 square; (f) Result of 3x3 mean filtering

LAB 06

Figure 1 shows two original images. From Lab exercise 5, noisy version of these images have been taken. Ideal lowpass filter and Butterworth lowpass filter are applied to the noisy images using two different cutoff frequencies of D_o=0.1 and $D_o = 0.6$.

(a)

(b)
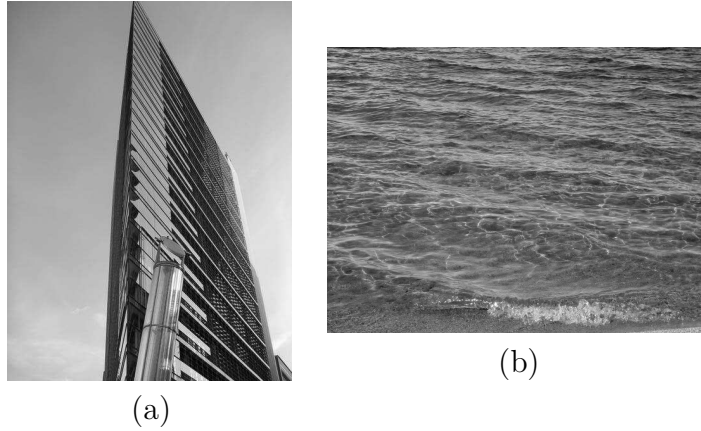
Figure 1: (a) An image with strong edges (b) An image with smooth features

Figure 2 shows the effect of applying ideal lowpass filter and Butterworth lowpass filter to the image of 1(a) at cutoff frequency D_o=0.1. The application of the lowpass filters have resulted in the suppression of noise, as seen in parts (c)-(f) of Figure 2. A glaring artifact is readily seen in the result of the ideal lowpass filter in figure 2(c) and 2(d). Faint echos of the edges present in the image have appeared in the result. This is due to the fact that the inverse Fourier transform of the circular ideal filter is a Bessel function. Multiplication of the Fourier transform of the image with the circle function is equivalent to convolution of the image in the space domain with the corresponding Bessel function. The ripples or lobes of the Bessel function lead to echos of strong edges, an artifact known as the ringing artifact. The Butterworth lowpass filter has suppressed the noise without causing the ringing artifact as seen in figure 2(e) and 2(f); however , the filter has caused some blurring of the edges of the image. Figure 3 shows the effect of applying ideal lowpass filter and Butterworth low pass filter to the image 1(a) at cutoff frequency D_o=0.6. It is seen that, in case of cutoff frequency D_o=0.1, the filtered images became more blurred than with cutoff frequency D_o=0.6. More details of the images are available with higher cut-off frequency as more high frequency contents are available in the image. Figure 4 and 5 shows the effect of applying ideal lowpass filter and Butterworth lowpass filter into image 1(b). The ideal lowpass filter has introduced some ringing artifact which is not present in case of Butterworth lowpass filter. For the images in figure 5 with higher cutoff frequency D_o=0.6, there are more details in the images. So we can conclude that, the ideal filter's abrupt transition from passband to stopband is not a desirable characteristic. The Butterworth filter's smooth transition from stopband to passband prevents the ringing artifact.
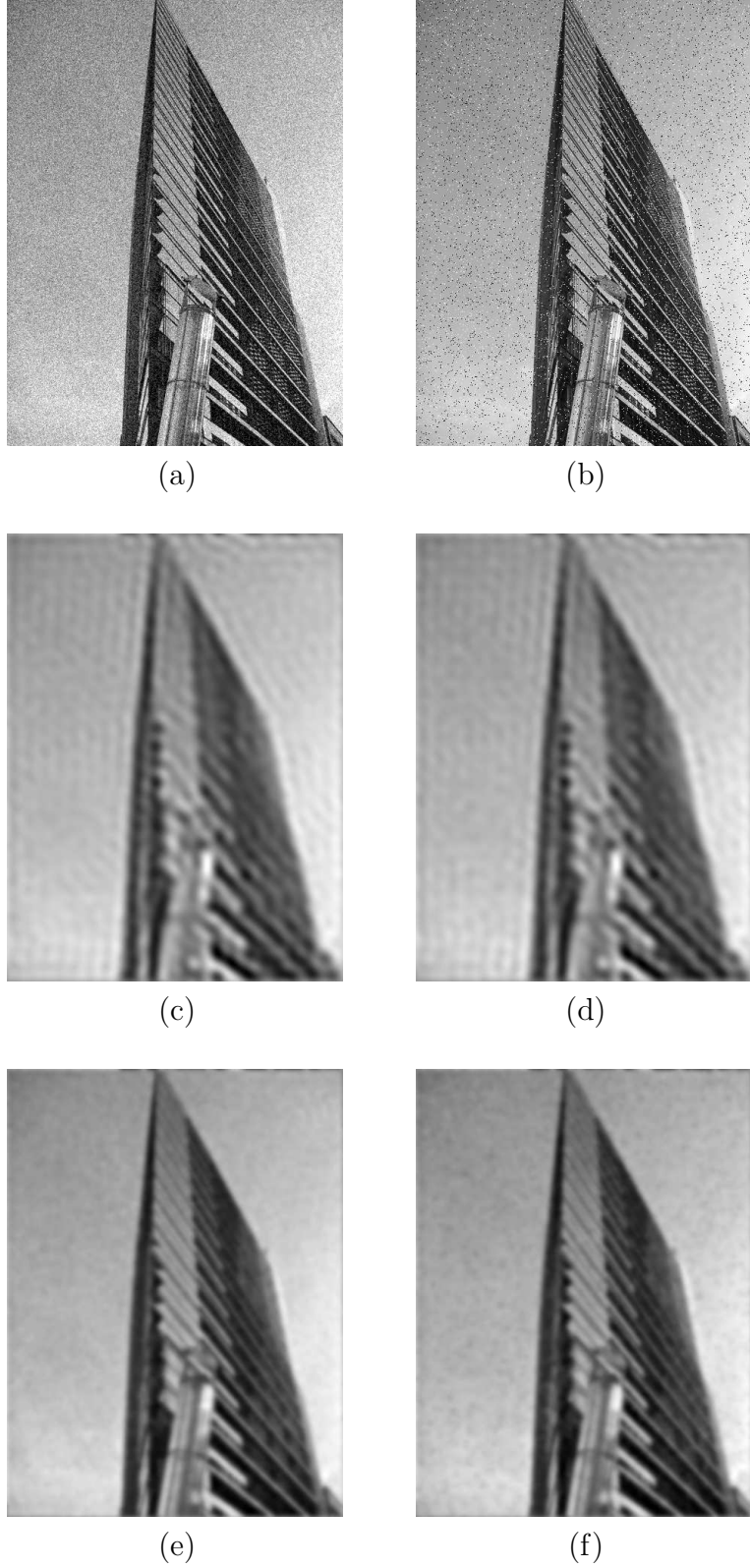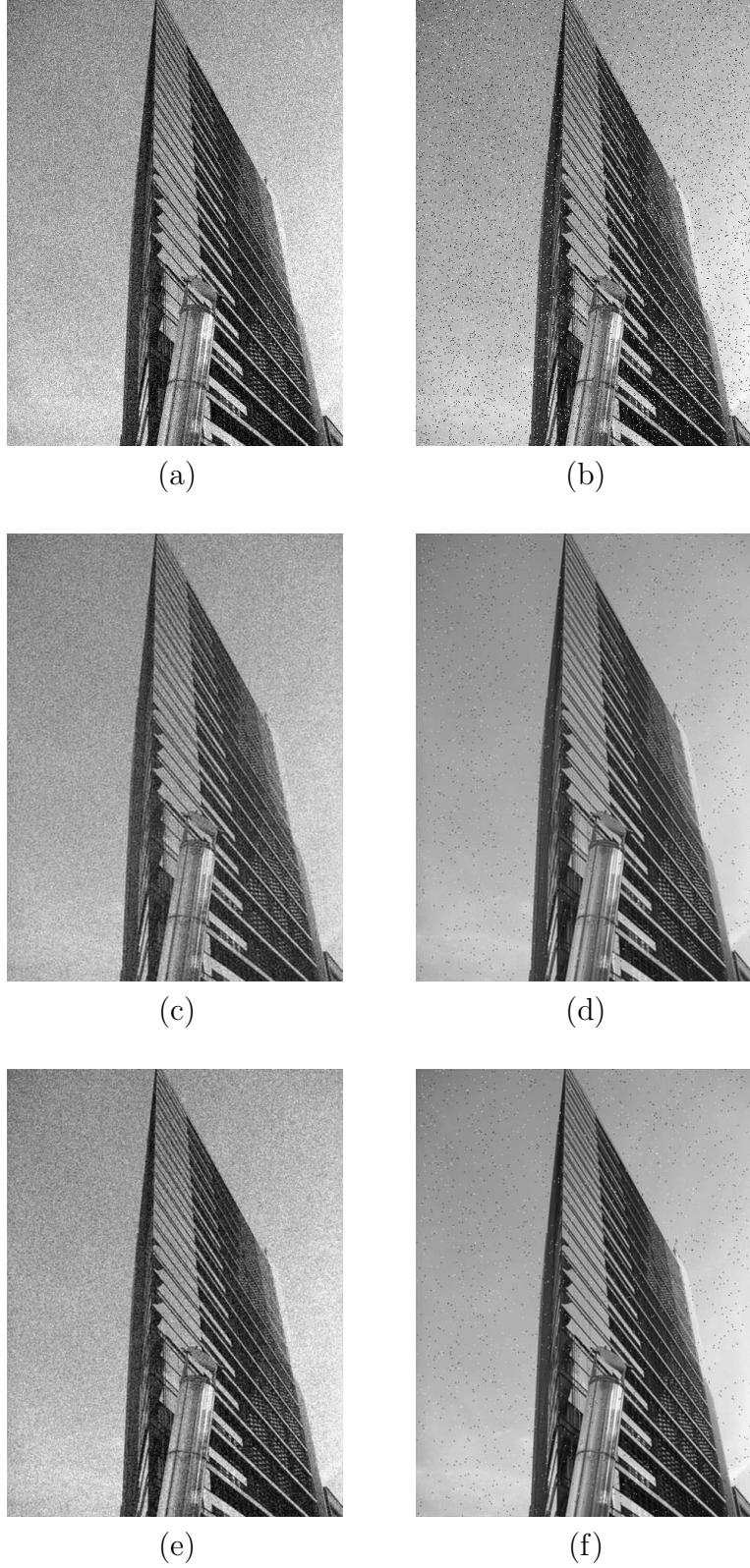
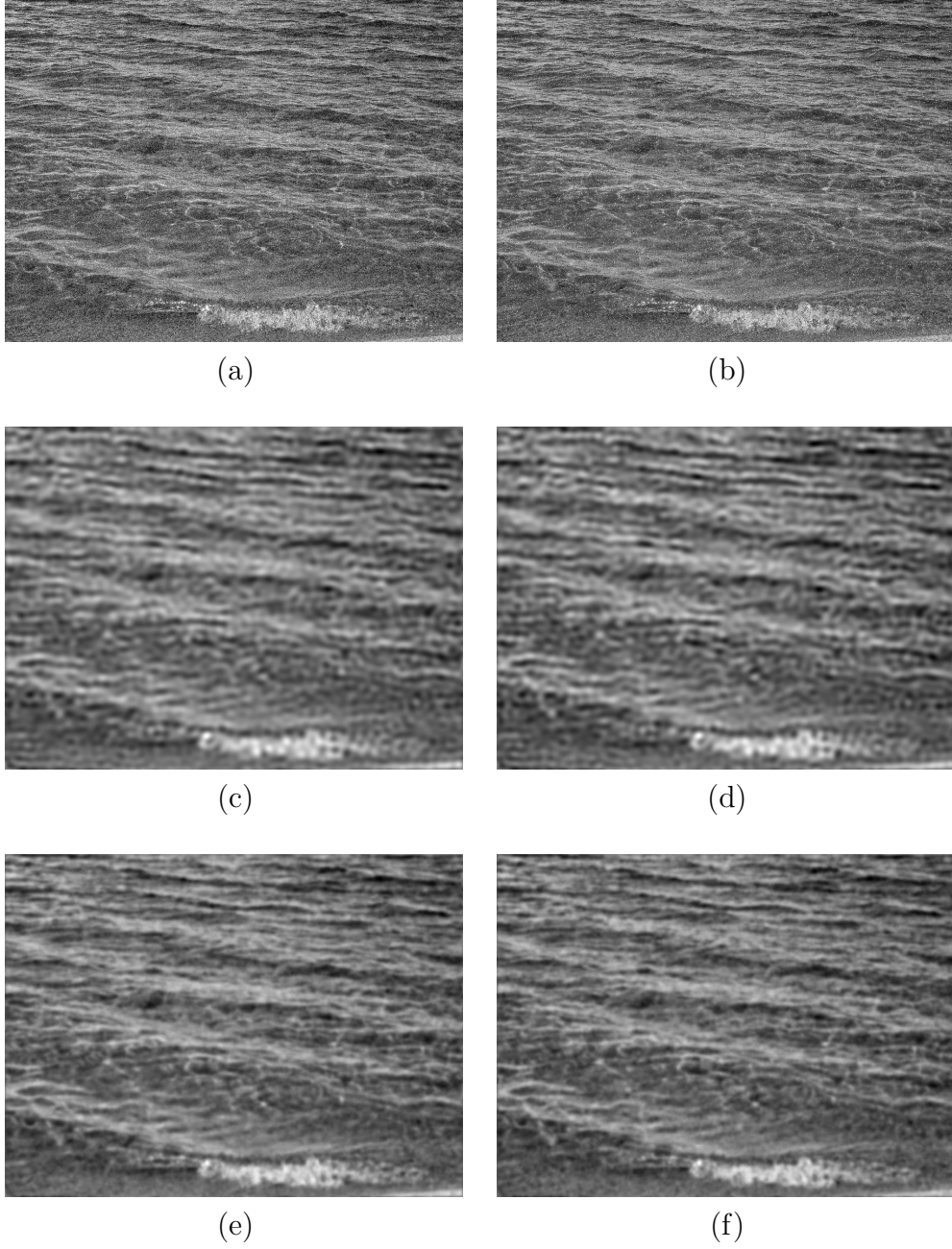Figure 2: Sharp edges:(a) Original image with Gaussian noise for μ=0, normalized σ^2=0.01; (b) Original image with salt and pepper noise for normalized σ^2=0.05; (c) Noisy image (a) filtered with ideal lowpass filter for D_o=0.10; (d) Noisy image (b) filtered with ideal lowpass filter for D_o=0.10; (e) Noisy image (a) filtered with Butterworth lowpass filter for D_o=0.10; (f) Noisy image (b) filtered with Butterworth lowpass filter for D_o=0.10
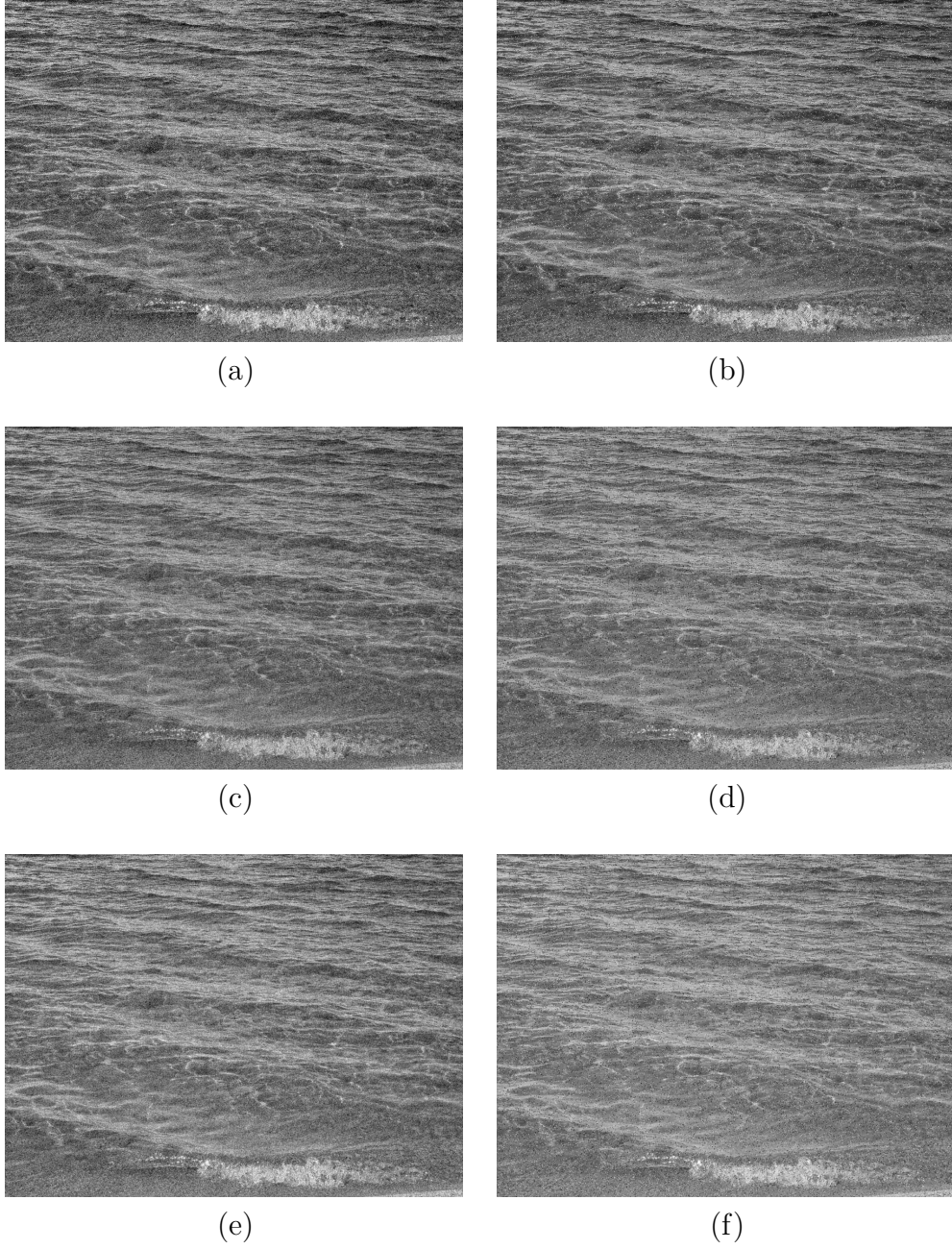
Figure 3: Sharp edges:(a) Original image with Gaussian noise for μ=0, normalized σ^2=0.01; (b) Original image with salt and pepper noise for normalized σ^2=0.05; (c) Noisy image (a) filtered with ideal lowpass filter for D_o=0.60; (d) Noisy image (b) filtered with ideal lowpass filter for D_o=0.60; (e) Noisy image (a) filtered with Butterworth lowpass filter for D_o=0.60; (f) Noisy image (b) filtered with Butterworth lowpass filter for D_o=0.60

Figure 4: (a) Original image with Gaussian noise for $\mu=0$, normalized $\sigma^2=0.01$; (b) Original image with salt and pepper noise for normalized $\sigma^2=0.05$; (c) Noisy image (a) filtered with ideal lowpass filter for $D_o=0.10$; (d) Noisy image (b) filtered with ideal lowpass filter for $D_o=0.10$; (e) Noisy image (a) filtered with Butterworth lowpass filter for $D_o=0.10$; (f) Noisy image (b) filtered with Butterworth lowpass filter for $D_o=0.10$

Figure 5: (a) Original image with Gaussian noise for $\mu=0$, normalized $\sigma^2=0.01$; (b) Original image with salt and pepper noise for normalized $\sigma^2=0.05$; (c) Noisy image (a) filtered with ideal lowpass filter for $D_o=0.60$; (d) Noisy image (b) filtered with ideal lowpass filter for $D_o=0.60$; (e) Noisy image (a) filtered with Butterworth lowpass filter for $D_o=0.60$; (f) Noisy image (b) filtered with Butterworth lowpass filter for $D_o=0.60$

LAB 07

Figure 1(a) displays a test image containing sharp edges. The effect of applying unsharp masking filter, the Laplacian operator and the subtracting Laplacian are seen in figure 1 (b)-(d). The unsharp masking filter has performed edge enhancement of the original image. But there is no net change in the image intensity. On the other hand, though the Laplacian operator has detected edges in all direction, it has removed the intensity information. There is a subtle border that surrounds the image and arises from zero-padding when the operator is applied near the edge of the image. The subtracting Laplacian has also performed edge enhancement of the original image like unsharp masking filter. The high frequency components are amplified as the gain increases quadratically with the frequency. The subtracting Laplacian has provided higher levels of sharpening than the unsharp masking filter. The unsharp masking filter and the subtracting Laplacian operator introduce disturbing overshoot and undershoot artifacts around edges, known as the ringing artifact. Although the artifact is not strongly evident in the images, the effect is, indeed, present.

Figure 2 shows the noisy version of the original image in figure 1(a) and the effects of applying the operators to the noisy image. In the presence of noise, as shown in (b), (c) and (d) of Figure 2, noise is emphasized by the operators. The effect of subtracting Laplacian is more noisy than that of the unsharp masking filter. Because in case of subtracting Laplacian, the high frequency is more amplified due to the increase of gain quadratically with the frequency. The effect of the Laplacian operator in the noisy image has made the image worst among the three operators. It has amplified the high frequency components and the shape of the original image is hardly visible.

Figure 3(a) displays a test image containing smooth features. The application of the Laplacian, part (c) of Figure 3, has removed all relative intensity information from the image, leaving only the high positive and negative values corresponding to the edges of the image. The unsharp masking filter and the subtracting Laplacian operator has enhanced the edges and the intensity of the image is also maintained. Though in case of the subtracting Laplacian operator, the image has become brighter. Figure 4(a) is the Gaussian noise added version of figure 3(a). As it is seen from the figures, all the operators have emphasized the noise. The effect of the Laplacian operator in the noisy image has made the image worst among the three operators as seen also in the previous image.
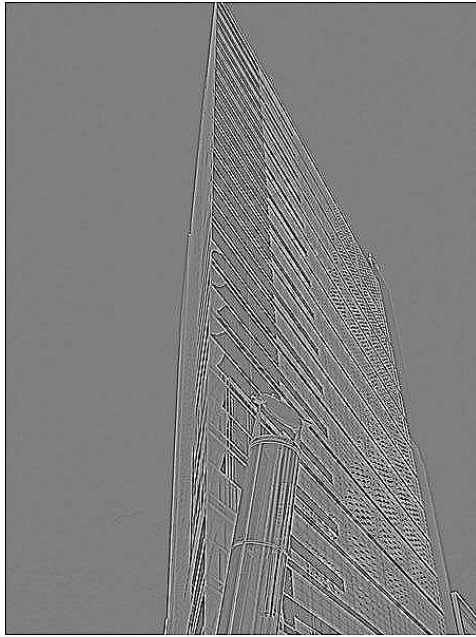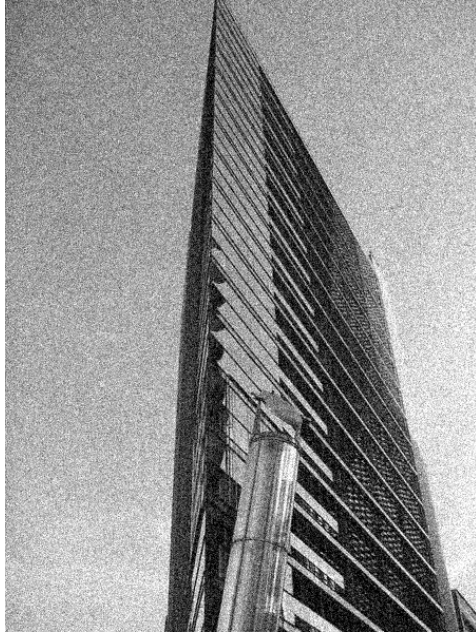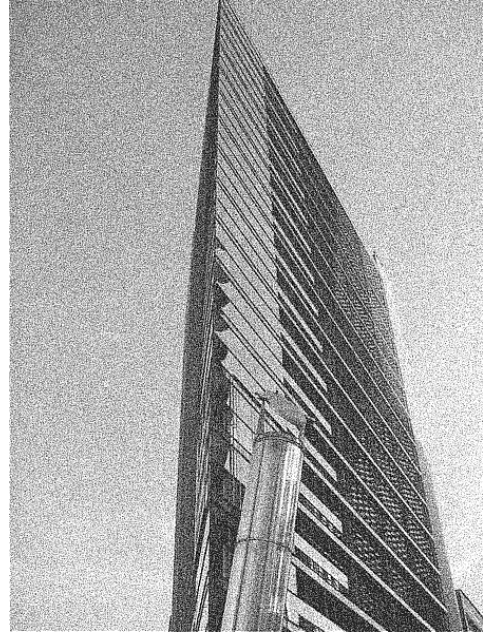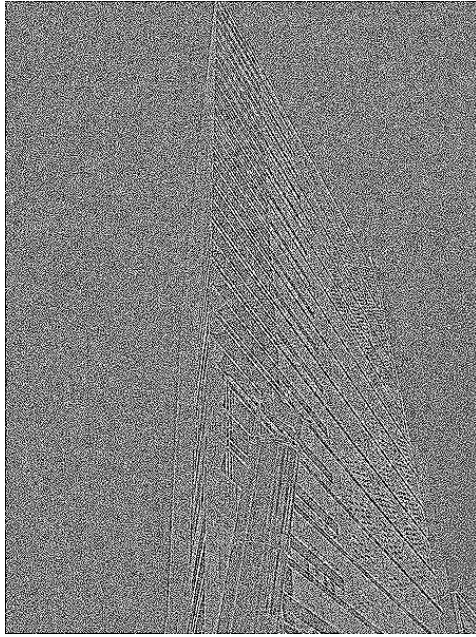
Figure 1: (a) Original image; (b) Unsharp mask applied to original image, display range [-50,250] out of [-94,360]; (c) Laplacian applied to original image, display range [-100,100] out of [-556,500]; (d) Subtracting Laplacian applied to original image, display range [-50,250] out of [-446,771]
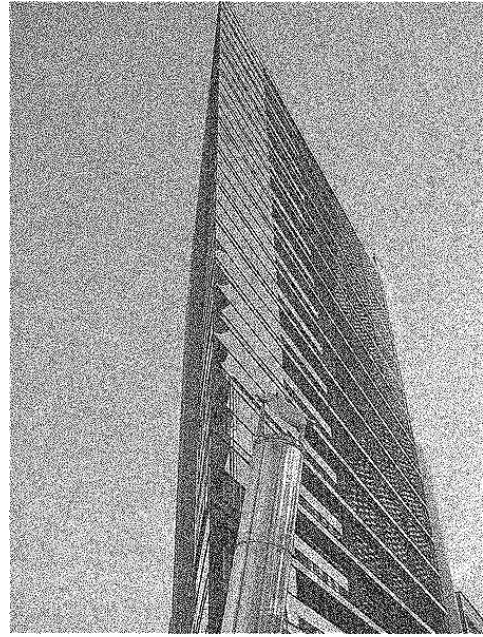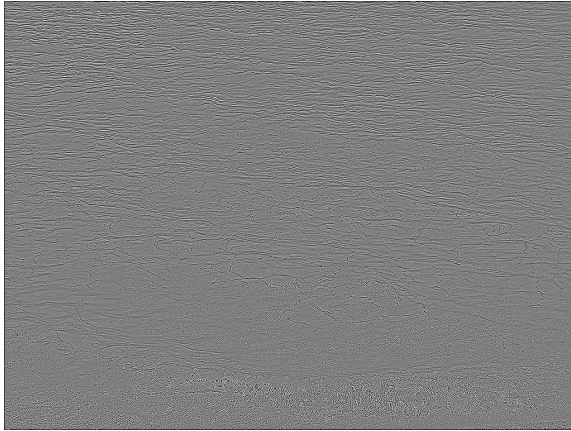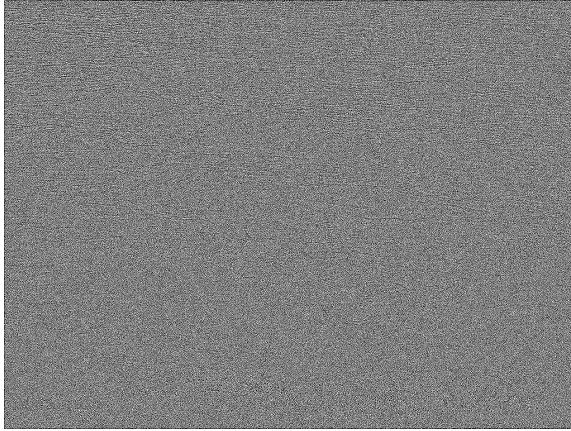
Figure 2: (a) Noisy image with Gaussian noise for normalized σ^2=0.01; (b) Unsharp mask applied to noisy image, display range [-50,250] out of [-145,425]; (c) Laplacian applied to noisy image, display range [-100,100] out of [-701,587]; (d) Subtracting Laplacian applied to noisy image, display range [-50,250] out of [-572,955]

(a)

(b)

(c)

(d)

Figure 3: (a) Original image; (b) Unsharp mask applied to original image, display range [50,250] out of [6,363]; (c) Laplacian applied to original image, display range [-100,100] out of [-434,245]; (d) Subtracting Laplacian applied to original image, display range [-50,250] out of [-141,662]

Figure 4: (a) Noisy image with Gaussian noise for normalized σ^2=0.01; (b) Unsharp mask applied to noisy image, display range [-50,250] out of [-124,424]; (c) Laplacian applied to noisy image, display range [-100,100] out of [-576,540]; (d) Subtracting Laplacian applied to noisy image, display range [-50,250] out of [-517,831]

LAB 08

Figure 1(a) shows a test image containing sharp edges. The effect of applying the ideal highpass filter, the Butterworth highpass filter and the Butterworth high-emphasis filter for cutoff frequency $D_o = 0.1$ has been shown in figure 1 (b)-(d). Although the ideal highpass filter has extracted the edges of the images, the strong presence of ringing artifacts diminishes the value of the result. Part (c) of the figure shows the result of the Butterworth highpass filter, where the edges are seen without the ringing artifact. The result of Butterworth high-emphasis filter, shown in part (d) of the figure, demonstrates edge enhancement; however, the relative intensities of the image has been altered.

Figure 2 shows the result of applying all the three filters at cutoff frequency $D_o = 0.4$. Due to higher cutoff frequency, more low frequency components are removed from the images. The ideal highpass filter still shows the ringing effect. Because the gain of a Butterworth highpass filter is zero at DC, the intensity information is removed by the filter. This leads to a result that depicts only the edges present in the image. Furthermore, the result will have positive and negative values. This phenomenon is easily visible in figure 2(c).The intensity information is still present in figure 2(d) for high-emphasis filter because it has a nonzero gain at DC. The parameters for the high-emphasis Butterworth filter, using the definition provided in the text, are κ_1=0.5 and κ_2=1.0.

Figure 3 shows the effect of the filters in the noisy version of the original image in 1(a) for cutoff frequency $D_o = 0.1$. In all the images, the high frequency noise has been emphasized. The ringing effect is visible in case of ideal highpass filter. The high-emphasis filter retains the intensity information while the highpass filter removes it. The effect of applying cutoff frequency $D_o = 0.4$ was also observed. At higher cutoff frequency, the low frequency components are eliminated.

Figure 4 shows the effect of three types of highpass filtering into a test image containing relatively smooth features for cutoff frequency $D_o = 0.1$. The ideal highpass filter has introduced ringing artifacts. The Butterworth highpass filter has removed the intensity information while the high-emphasis filter retained the information. The effect of filtering on the noisy version of the original image in figure 4 (a) was also observed. In all cases the noise was amplified. The effect of applying cutoff frequency $D_o = 0.4$ was also observed. In case of lower cutoff frequency, there was more details while the higher cutoff frequency eliminated details from the images.

So from the above discussion, we can conclude that, the ideal highpass filter extracted the edges with some ringing artifact. The Butterworth highpass filter extracted the edges without having any ringing artifact, but the intensity information was removed. The Butterworth high-emphasis filter enhanced the edges retaining the intensity information of the original image.
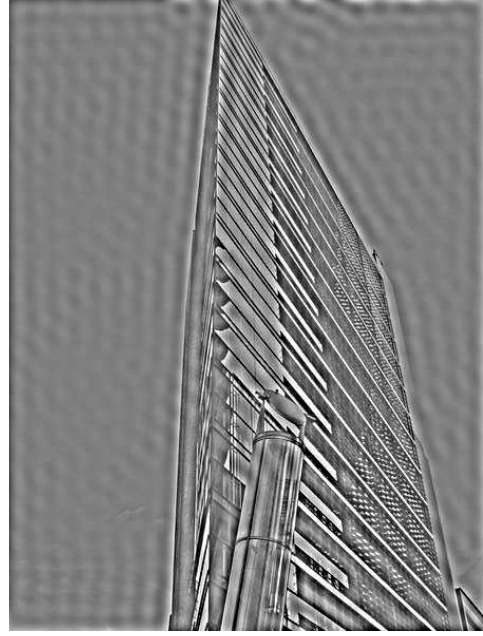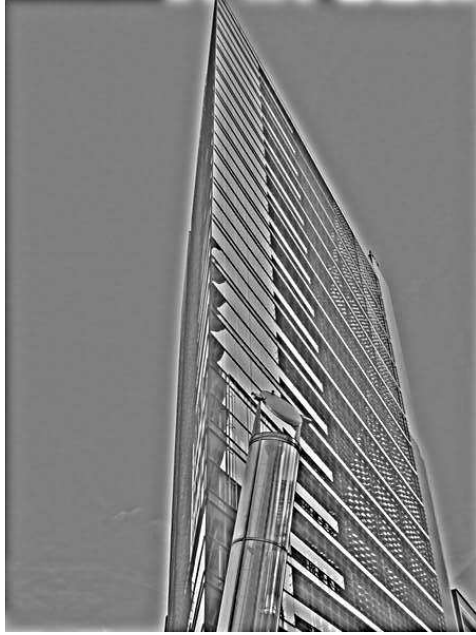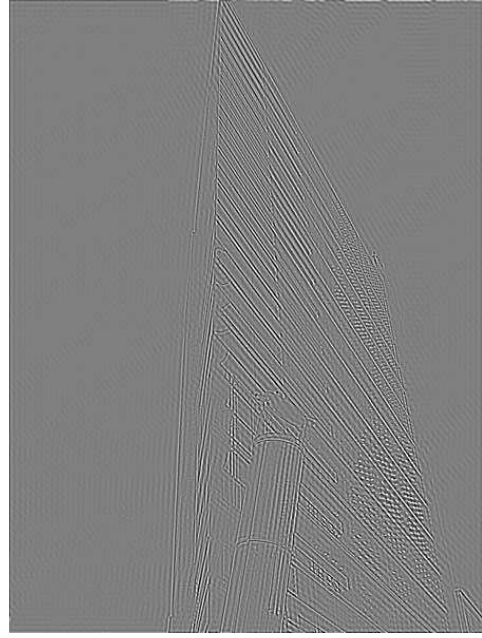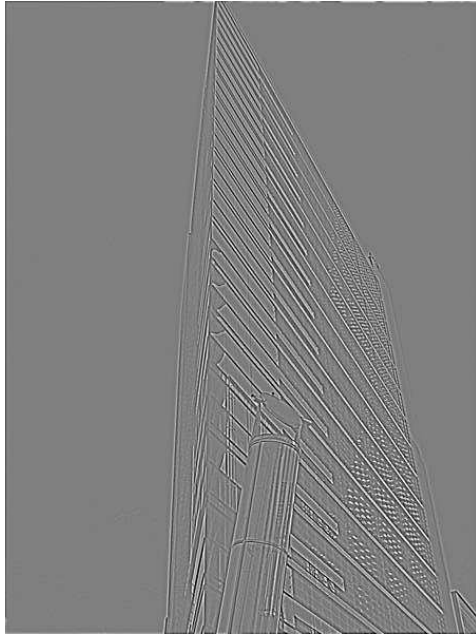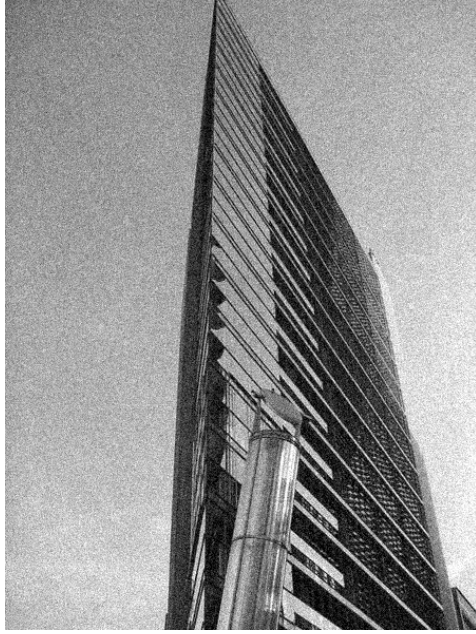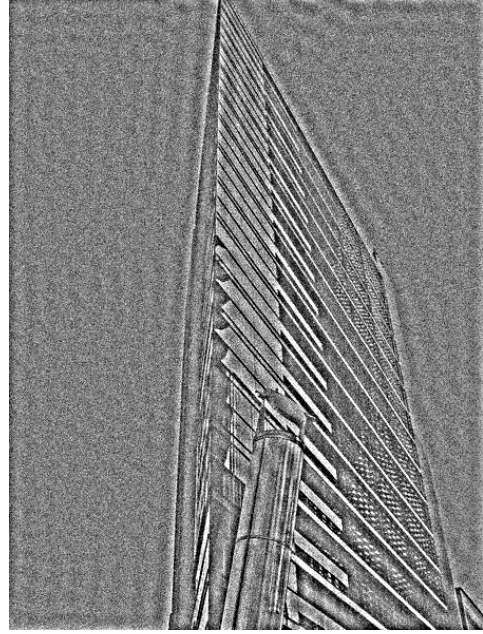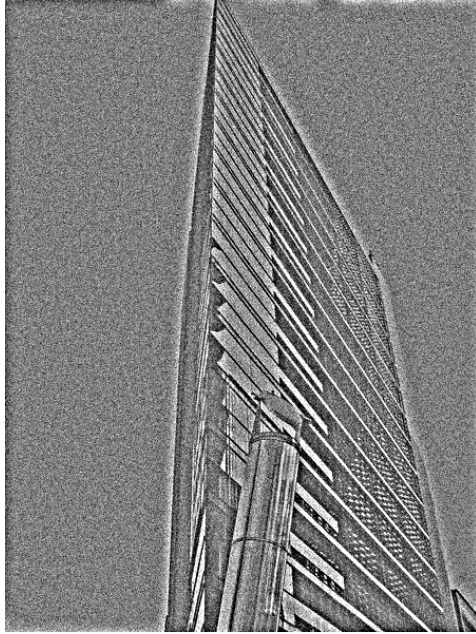
Figure 1: For cutoff frequency $D_o = 0.1$ (a) Original image; (b) Ideal highpass filter applied to original image, display range [-80,80] out of [-140.63,169.96]; (c) Butterworth highpass filter applied to original image, display range [-80,80] out of [-162.49,179.86]; (d)Butterworth high emphasis filter applied to original image, display range [-80,140] out of [-131.63,288.01]

Figure 2: For cutoff frequency $D_o = 0.4$ (a) Original image; (b) Ideal highpass filter applied to original image, display range [-80,80] out of [-108.09,125.23]; (c) Butterworth highpass filter applied to original image, display range [-80,80] out of [-112.20,132.05]; (d) Butterworth high emphasis filter applied to original image, display range [-80,140] out of [-97.09,237.23]

(a)

(b)

(c)

(d)

Figure 3: For cutoff frequency $D_o = 0.1$ (a) Noisy image with gaussian noise for normalized σ^2=0.005; (b) Ideal highpass filter applied to noisy image, display range [-80,80] out of [-157.96,190.57]; (c) Butterworth highpass filter applied to noisy image, display range [-80,80] out of [-180.14,212.04]; (d) Butterworth high emphasis filter applied to noisy image, display range [-80,140] out of [-157.96,313.37]

(a)
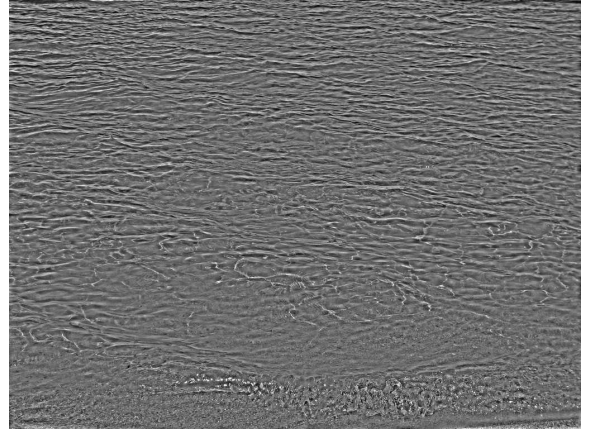
(b)
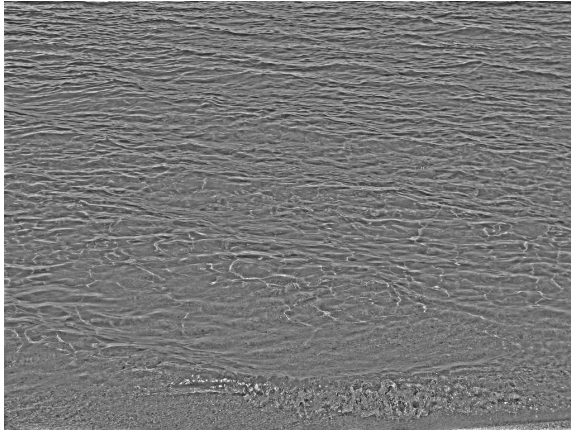
(c)

(d)

Figure 4: For cutoff frequency $D_o = 0.1$ (a) Original image; (b) Ideal highpass filter applied to original image, display range [-60,80] out of [-75.49,123.68]; (c) Butterworth highpass filter applied to original image, display range [-70,80] out of [-79.33,128.78]; (d)Butterworth high emphasis filter applied to original image, display range [-20,140] out of [-44.76,251.18]

5

LAB 09

Two images figure 1 (a) and (c) have been selected from the collection of images, containing objects with gray levels that are well separated from the gray levels of the background. The MAT-LAB command graythresh is used for thresholding and im2bw is used to binarize the thresholded images. The effect of thresholding and binarization of images 1 (a) and (c) is shown in figure 1 (b) and (d) respectively.

In figure 1 (a) a normalized thresholding level of 0.4471 was used. It is seen from figure 1 (b) that the gray levels below this threshold has been considered as black and above the threshold as white. As the background was brighter than the building, it has become complete white. The darker portions of the building has become black. So the object is easily separated from the background.

In figure 1(c) a normalized thresholding level of 0.4784 was used. In this figure the object was brighter than the background. So after thresholding and binarization, the dark background has become black and the baby has become white except the eyes, hair and the edges of the face.
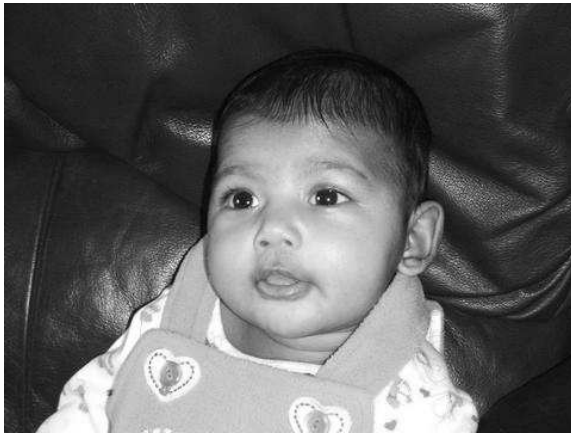
The performance of the methods is exceptionally well for the first image. In case of the second image also the result is acceptable. But still for both images, edge detection and post-binarization together may improve the segmentation of the objects from their background. Mathematical morphology could also be used to improve the result.

(a)   (b)

(c)   (d)

Figure 1: (a) Original image of sharp edges; (b) Result of thresholding image (a) at normalized level 0.4471; (c) Original image of a baby face; (d) Result of thresholding image (c) at normalized level 0.4784

LAB 10

Figure 1(a) is a test image with strong edges of the objects or features in the image. The result of application of the 3x3 Prewitt operators for 0, 45, 90 and 135 degrees on image 1(a) has been depicted in figure 1 (b)- (e) respectively. Part (f) of the figure shows the gradient magnitude image, obtained by combining the horizontal and vertical derivatives, shown in part (b) and (d) of the figure respectively. The gradient magnitude operation can be used for edge detection where the object boundary at all directions are desired. The image in part (b) presents high values (positive or negative) at vertical edges only; horizontally oriented edges have been deleted by the horizontal derivative operator. The image in part (d) shows high output at horizontal edges, with the vertically oriented edges having been removed by the vertical derivative operator. Part (c) and (e) of the figure show the derivatives at 45 degree and 135 degree respectively; the images indicate the diagonal edges present in the image.

Figure 2 (a) is a test image with weaker definition of edges and features. The result of application of the 3x3 Prewitt operators for 0, 45, 90 and 135 degrees on image 2(a) has been depicted in figure 2 (b)- (e) respectively. Part (f) of the figure shows the gradient magnitude image, obtained by combining the horizontal and vertical derivatives, shown in part (b) and (d) of the figure respectively. It can be seen that the various Prewitt direction operators do an excellent job of detecting, or rather eliminating the appropriate edges from the image.

In lab exercise 4, the horizontal and vertical derivative of image 1(a) and 2(a) were computed. By comparing the images of first order derivative with these images, it is found that, the result of edge detection with the Prewitt operators are more accurate. The horizontal and vertical operators are based on only two pixel values which make them more susceptible to noise. The Prewitt operators provide more reliable edge detection. The double edge visible in Laplacian operator is removed here and the edges can be extracted at any particular orientation.
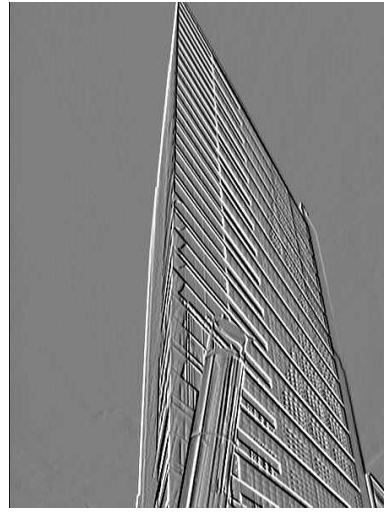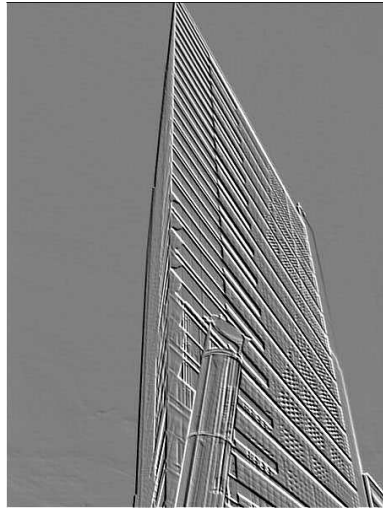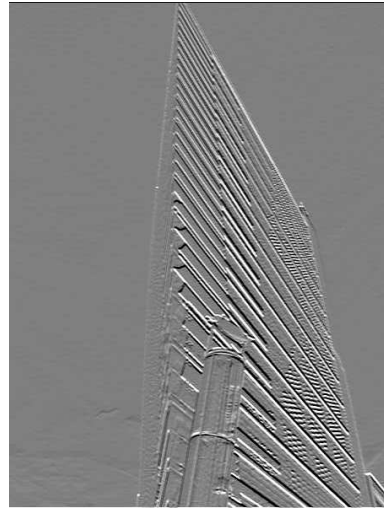
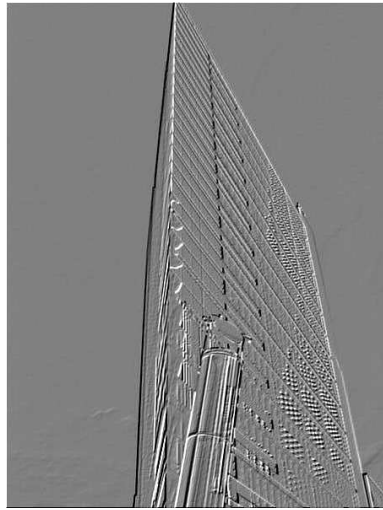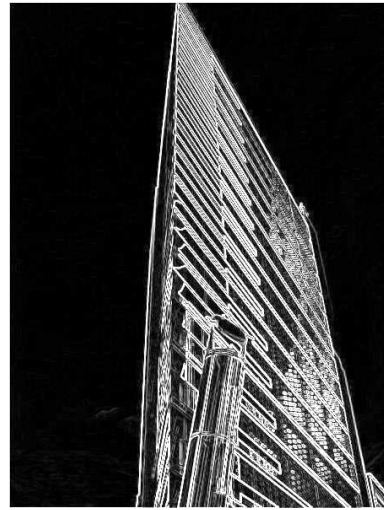Figure 1: (a) Original image of sharp edges; Result of Prewitt operators ; (b) For 0 degree, display range [-200,200] out of [-592,732]; (c) For 45 degree, display range [-200,200] out of [-602,662]; (d) For 90 degree, display range [-200,200] out of [-503,694]; (e) For 135 degree, display range [-200,200] out of [-568,436]; (f) The magnitude of the gradient, display range [0,200] out of [0,732]
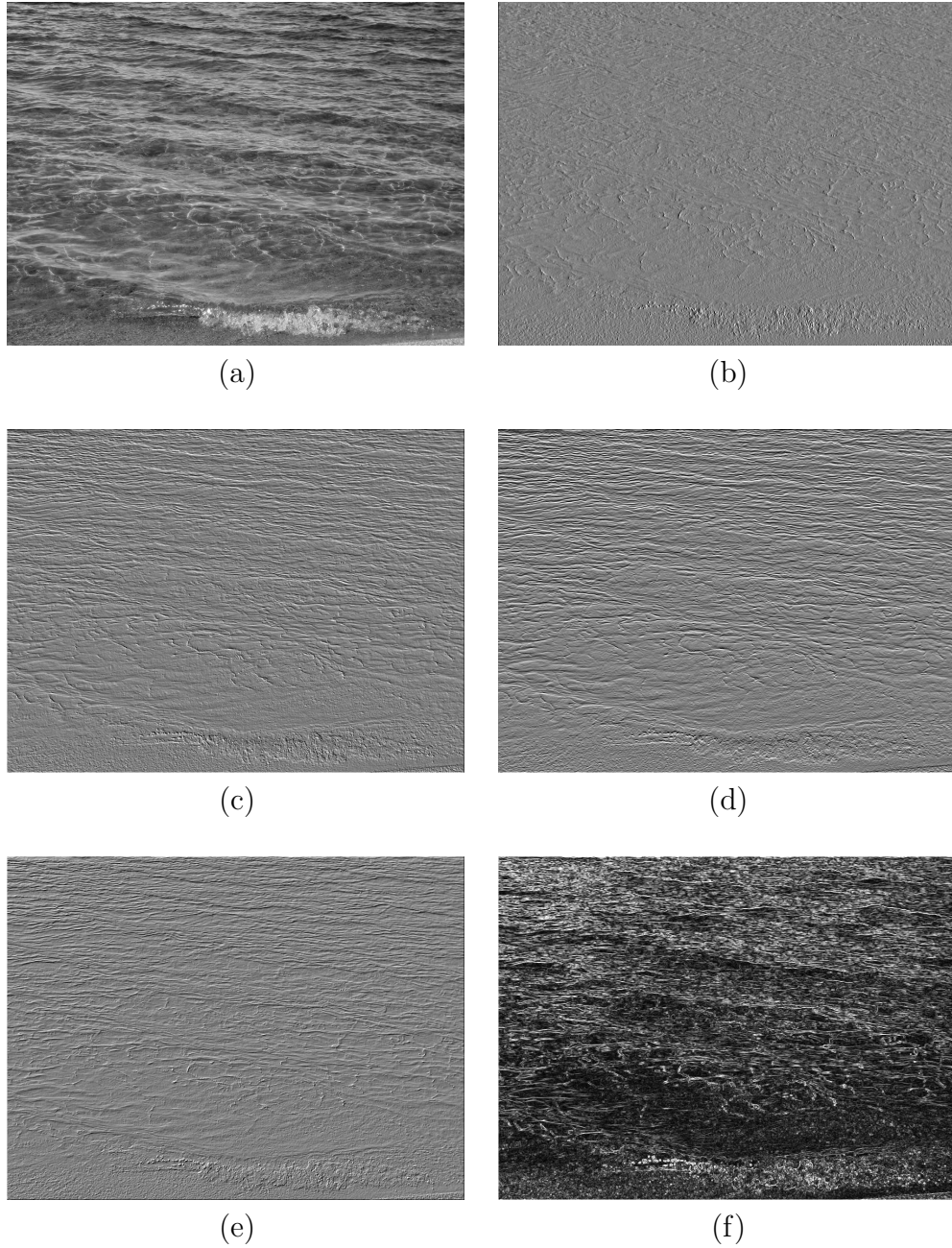
2

Figure 2: (a) Original image of weaker definition of edges; Result of Prewitt operators ; (b) For 0 degree, display range [-200,200] out of [-589,586]; (c) For 45 degree, display range [-200,200] out of [-408,514]; (d) For 90 degree, display range [-200,200] out of [-592,654]; (e) For 135 degree, display range [-200,200] out of [-589,453]; (f) The magnitude of the gradient, display range [0,200] out of [0,659.76]